# A G-Quadruplex Aptamer Inhibits the Phosphatase Activity of Oncogenic Protein Shp2 in vitro

**ARTICLE** *in* CHEMBIOCHEM · FEBRUARY 2011

Impact Factor: 3.09 · DOI: 10.1002/cbic.201000470 · Source: PubMed



**8 AUTHORS**, INCLUDING:

Wei Yun Zhang
Xiamen University
**20** PUBLICATIONS **343** CITATIONS
SEE PROFILE

Zhongxian Lu
Xiamen University
**21** PUBLICATIONS **427** CITATIONS
SEE PROFILE

Chaoyong James Yang
Xiamen University
**123** PUBLICATIONS **4,601** CITATIONS
SEE PROFILE

CHEMBIOCHEM

DOI: 10.1002/cbic.201000470

# A G-Quadruplex Aptamer Inhibits the Phosphatase Activity of Oncogenic Protein Shp2 in vitro

Jia Hu,[a] Jie Wu,[a] Cong Li,[a] Ling Zhu,[a] Wei Yun Zhang,[a] Guiping Kong,[b] Zhongxian Lu,*[b] and Chaoyong James Yang*[a]

Shp2 is a member of the protein tyrosine phosphatase (PTP) family, which regulates a variety of cellular processes including cell growth, differentiation, mitotic cycle, and oncogenic transformation. Using a recombinant Shp2-GST protein as the target and GST as a counter target, we have identified two classes of single-stranded DNA aptamers that selectively bind to Shp2 with a $K_d$ in the nanomolar range. Structural studies of the most abundant sequence in the enriched library, HJ24, revealed a parallel G-quadruplex as the core binding domain. Furthermore, this aptamer was found to be an effective inhibitor of Shp2 phosphatase, an effect which was readily reversed by using the cDNA of HJ24. In view of these characteristics, this aptamer has the potential to be used for further development of Shp2 assays and therapeutics for the treatment of Shp2-dependent cancers and other diseases.

## Introduction

Reversible tyrosyl phosphorylation, which is controlled by protein tyrosine kinases (PTKs) and protein tyrosine phosphatases (PTPs), regulates numerous signaling events that are fundamental to virtually all essential cellular processes. Altered expression and/or mutations in PTKs and PTPs result in aberrant tyrosine phosphorylation, which has been linked to several human diseases, including cancer.[1–3] A member of the PTP family, the SH2 domain-containing phosphatase Shp2, was discovered in the early 1990s and is regarded as a bona fide oncogene.[4] Since its discovery, Shp2 has been established as a critical contributor to the signaling pathways of many important kinases including Ras-MAPK, Jak-Stat, and PI3K-AKT, regulating a broad range of cellular processes including proliferation, differentiation, migration, apoptosis, and immune responses.[5,6] It is well established that dysfunction of Shp2 is associated with cancers, metabolic syndromes, and autoimmune disorders.[7–14] Especially in cancer, Shp2 is mutated in several types of leukemia and hyperactivated by other mechanisms in some solid tumors. However, many important questions remain about normal Shp2 functions and how its perturbation leads to human disease. Understanding how Shp2 and other PTPs contribute to oncogenesis would provide new insights into pathogenesis and might suggest new targets for antineoplastic drugs. Consequently, design of a selective molecular probe that binds Shp2 with high affinity and excellent selectivity will be of great significance to delineate the physiological roles of the protein. Moreover, the screening of inhibitors to the PTP domain of Shp2 has become an active research area for therapeutic development.

Aptamers are a new class of molecular probes that have attracted intense attention. They are single-strand oligonucleotides that can recognize a wide variety of molecules ranging from small organic species to proteins.[15–17] They are obtained from an in vitro screening technique termed SELEX (system evolution of ligands by exponential enrichment),[18,19] which involves progressive selection of aptamers by repeated rounds of partitioning and amplification from a combinatorial oligonucleic acid library. Aptamers have many important attributes including high affinity and specificity for their targets, quick and reproducible synthesis, flexible modification, biocompatibility, low toxicity, and in vitro stability.[20–22] These advantages make aptamers promising ligands for medical and pharmaceutical research, drug development, diagnosis and therapy.[23–28]

In this study, using recombinant Shp2, we have identified two classes of single-stranded DNA aptamers that selectively bind to Shp2 with high affinity. Structural studies on one of the aptamer sequences, HJ24, revealed a parallel G-quadruplex as the core binding domain. By interaction with Shp2, HJ24 was shown to inhibit phosphatase activity. These characteristics render the aptamer a promising tool to study Shp2 function and a potential therapeutic agent applicable for the selective control of Shp2 phosphatase activity.

[a] J. Hu, J. Wu, C. Li, L. Zhu, Dr. W. Y. Zhang, Prof. C. J. Yang
State Key Laboratory for Physical Chemistry of Solid Surfaces
The Key Laboratory for Chemical Biology of Fujian Province
Key Laboratory of Analytical Sciences and Department of Chemical Biology
College of Chemistry and Chemical Engineering, Xiamen University
Xiamen 361005 (China)
Fax: (+86) 592-2189959
E-mail: cyyang@xmu.edu.cn

[b] G. Kong, Prof. Z. Lu
Institute for Biomedical Research, Xiamen University
Xiamen 361005 (China)
E-mail: zhongxian@xmu.edu.cn

Supporting information for this article is available on the WWW under http://dx.doi.org/10.1002/cbic.201000470.

## Results and Discussion

### FACS-SELEX for aptamers against protein

Figure 1 illustrates the process of selecting DNA aptamers for the protein Shp2. Recombinant Shp2 was fused with glutathione-S-transferase (GST) to facilitate attachment of the protein to solid supports (Sepharose beads) without the need for complicated conjugation chemistry. The highly hydrophilic nature of the Sepharose surface minimizes nonspecific binding of DNA to surfaces, ensuring systematic enrichment of target binding sequences. In addition, the mean size of Sepharose beads is about 34 μm, a diameter that is compatible with FACS analysis. Instead of using the tedious, time-consuming and radioactive EMSA process to monitor the progress of selection, FACS has been proven a simple, yet effective method of characterizing DNA–target binding affinity.[29–34] More importantly, during selection, by incubating Shp2-GST beads with the DNA library in binding buffer, proteins and DNA can interact in the solution phase; this allows effective binding to take place. Furthermore, beads can be washed thoroughly to remove nonspecific binders. To avoid the enrichment of DNA sequences that bind to GST or bead surface, GST beads were used as a negative control in the selection. In our selection, a library of ssDNAs that contained a 40-mer random sequence region flanked by two 20-mer PCR primer sequences was used. The library was first allowed to interact with excess negative control beads, and only the DNA sequences not bound to the beads were collected. The collected sequences were then incubated with Shp2-GST-beads to allow binding to take place. After washing, the bead–ssDNA complexes were collected, and the DNA was PCR amplified for the next round of selection. To increase the stringency of the selection, the DNA/protein ratio was gradually decreased while increasing the strength of washing to evolve strong binding sequences. After multiple rounds of selection, the subtraction process efficiently reduced the DNA sequences that bound to the control beads, while those Shp2-specific aptamer candidates were enriched.

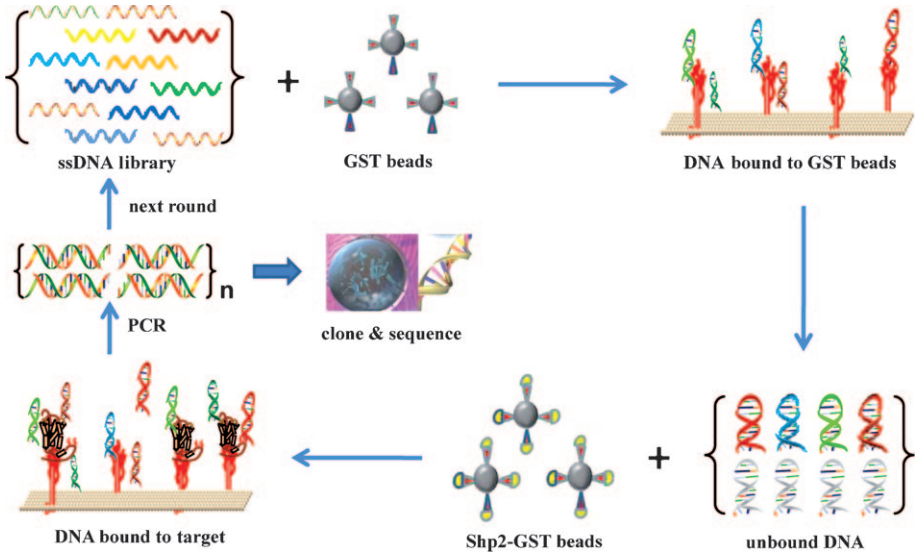


**Figure 1.** Sepharose-bead-based SELEX process for protein Shp2. The bead-immobilized Shp2-GST fused protein was incubated with the ssDNA library, which consists of about $10^{15}$ unique sequences in the desired buffer condition. To ensure highly stringent binding conditions, the ssDNA/protein ratio was initially kept at 100:1. After washing, the eluted DNAs were incubated with GST-coated Sepharose beads for counter-selection to remove sequences that bind to GST or bead surface. The ssDNA/GST ratio was 10:1. The Shp2-specific DNA sequences were subsequently amplified by PCR for the next round of selection, or for cloning and sequencing to identify individual aptamers after fluorimetric analysis.

The progress of the selection process was monitored by flow cytometry. The DNA products collected after each round were labeled with FAM dye by using FAM-labeled forward primer and incubated with Shp2-beads. The fluorescence intensity of the labeled beads measured by flow cytometry represented the binding capacity of the enriched DNA pool to the Shp2-beads. The stronger binding of the DNA library to Shp2, the more FAM-labeled sequences bound to the beads. With the increasing number of selection cycles, steady increases in fluorescence intensity on the positive beads were observed (Figure 2A); this indicated that DNA sequences with higher binding affinity to the target were enriched. In contrast, there was no significant change in fluorescence intensity on the control beads. After ten rounds of selection, the mean fluorescence intensity of the beads was 130 times higher than that of the initial library. The affinity of the enriched library after ten rounds of selection was found to be in the nanomolar range ($K_d = 16 \pm 4$ nM), while there was no observable binding of the library to control beads (Figure 2B). These results suggested that the DNA probes specifically recognizing Shp2 were enriched.

### Binding affinity of selected aptamers to Shp2

After ten rounds of selection, the enriched DNA pool was cloned and sequenced. The sequencing data for clones were analyzed by using sequencing analysis software ClustalW. The sequences were grouped based on the homology of the DNA sequences of individual clones with each group containing very similar sequences. Among 48 clones, there were two subfamilies each containing multiple sequences with high similarity. The sequence with the largest population, HJ24, appeared 13 times. The second largest population had 12 sequences with good similarity. HJ24 was selected and synthesized for further characterization. As shown in Figure 3, HJ24 can bind Shp2 with high affinity ($K_d = 11 \pm 4$ nM). Titration of HJ24 to

  

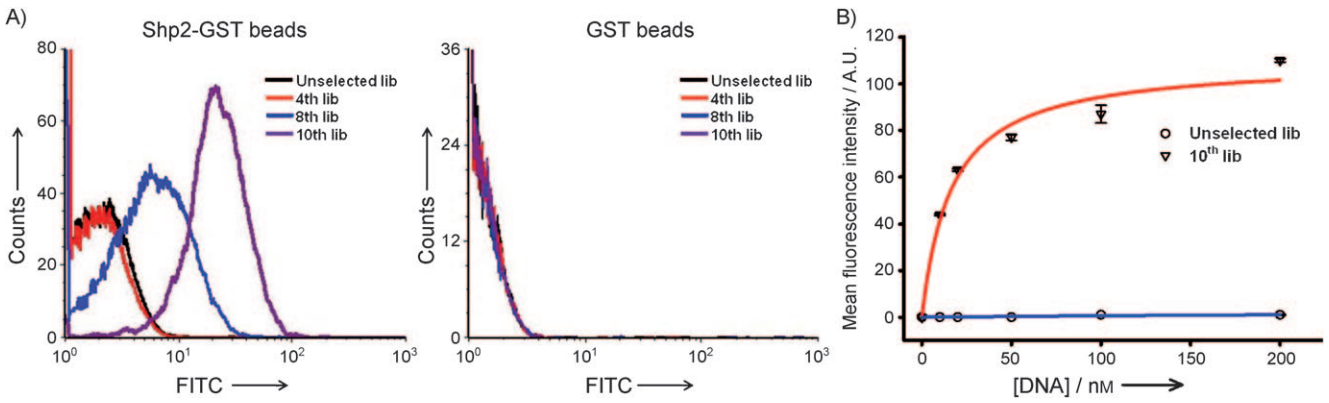


**Figure 2.** Enrichment of DNA sequences that bind to Shp2-GST-beads. A) Flow cytometry assay to monitor the binding of a selected pool with Shp2 (target protein) and GST (control protein). The black curve represents the background binding of unselected library. For the target protein Shp2, there was an increase in binding capacity of the pool as the selection progressed, while there was no observable change for the control protein GST. The final concentration of the selected pool in binding buffer was 100 nM. B) Determination of the dissociation constant of the enriched library to Shp2.

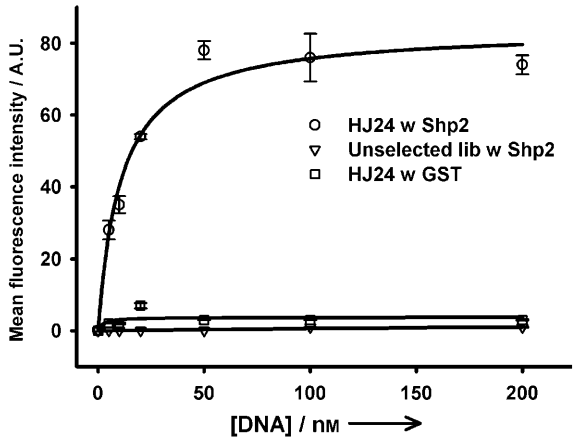


**Figure 3.** Fluorescence measurements to determine dissociation constant of selected aptamer HJ24. Two different negative controls were carried out. Negligible binding was observed between 1) the initial library and Shp2-GST beads (▽), 2) enriched aptamer HJ24 and GST beads (□).

GST beads revealed no observable binding of the DNA to GST; this established that the binding target of HJ24 was Shp2. Sequences from the second largest subfamily were synthesized, and similar binding constants to Shp2 were found.

### Aptamer HJ24 is a G-quadruplex

Further examination revealed that HJ24 has multiple stretches of guanines (AGC GTC GAA TAC CAC TAC AGG GGG TTT TGG TGG GGG GGG CTG GGT TGT CTT GGG GGT GGG CTA ATG GAG CTC GTG GTC AT). Guanine-rich sequences of nucleic acids can fold into four-stranded secondary structures called quadruplexes. Many DNA aptamers have been found to have guanine quadruplex (G-quartet) structure.[35–37] In the G-quadruplex, the planar square arrangement of four guanines (a tetrad) is stabilized by Hoogsteen hydrogen bonding. It is well established that the existence of a monovalent cation (especially potassium) in the center of these tetrads can significantly stabilize G-quadruplexes.[38–41] Depending on the direction of the strands or parts of a strand that form the tetrads, structures may be described as parallel or antiparallel. These quadruplexes can form through the intermolecular association of four or two DNA molecules, or by the intramolecular folding of a single strand containing four blocks of guanines.[42]

CD experiments were performed to investigate the secondary structure of HJ24. The CD spectrum of the HJ24 aptamer showed a negative peak near 240 nm and a positive peak near 260 nm (Figure 4A), a typical spectrum of a parallel G-quadruplex. To confirm the formation of the aptamer as a G-quartet structure, several additional experiments were performed. Firstly, replacing the longest G stretch (GGG GGG GG) in the aptamer with a scrambled sequence (AAC TGA CT) led to the disappearance of the 260 nm peak in the CD spectrum (Figure 4A). Secondly, all peaks in the spectra were dependent on $K^+$ ions but not $Mg^{2+}$, a typical characteristic of a G-quadruplex (Figure 4B). These results suggest that it is highly possible that HJ24 forms a parallel G-quadruplex structure.

In general, the majority of parallel G-quadruplexes form through intermolecular association. To investigate whether HJ24 forms intermolecular four-stranded or intramolecular single-stranded G-quadruplex structures, the dependence of melting temperature on the concentration of HJ24 was studied. The melting temperature of HJ24 was found to be 58 °C at 295 nm, which was independent of oligonucleotide concentration (Figure 5); this indicates that the aptamer forms an intramolecular G-quartet.[43]

### Effect of ions on structural stability of HJ24 and its binding affinity

It is well established that the existence of a monovalent cation (especially potassium) in the center of the tetrad can significantly stabilize a G-quadruplex. We further investigated how a cation would affect the structural stability and potentially the binding activity of HJ24. As shown in Figure 6A, the stability of the HJ24 G-quadruplex structure is strongly dependent on the nature of the monovalent ion. With 60 mM of KCl, strong CD

  

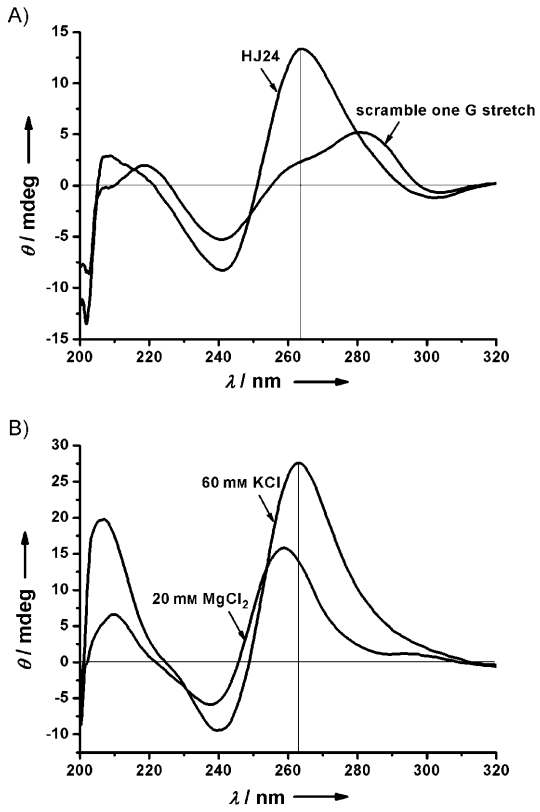


**Figure 4.** Characterization of the aptamer HJ24 by CD. A) The CD spectra of the aptamer HJ24 and its mutant sequence are shown. This aptamer has a positive band near 260 nm that can be assigned to parallel-strand quadruplex structures. There was no typical peak at 260 nm when altering the longest G stretch with a scrambled sequence of the same length. B) The CD spectra of the aptamer HJ24 in the presence of 60 mM KCl and 20 mM $MgCl_2$ are shown. The intensities of the peaks at around 210, 240, 260 nm in the presence of $MgCl_2$ were obviously lower than those in the presence of KCl.

peaks were observed, suggesting the formation of stable G-quartet structure. Replacing KCl with the same concentration of NaCl led to a dramatic decrease in CD intensity; replacing KCl with the same concentration of LiCl led to a further loss of this spectroscopic signature of the sequence. The effect of ions on the stability of the G-quadruplex is $K^+ > Na^+ > Li^+$, which is consistent with other G-quadruplexes.[43]

We further studied the effect of $K^+$ concentration on the stability of the G-quadruplex. As shown in Figure 6B, addition of 1 mM $K^+$ in phosphate buffer dramatically increased the CD intensity at 240 and 260 nm. CD absorption intensity increased with the increase of $K^+$ concentration and reached a plateau when $[K^+]$ was higher than 20 mM.

The binding affinity of HJ24 at different concentrations of $K^+$ was investigated. As shown in Figure 6C, very weak binding was observed when there was no $K^+$ in the buffer. The binding affinity of HJ24 significantly increased with the presence of $K^+$. The results demonstrated that formation of a G-quadruplex is important for the binding of aptamer to its target.

### HJ24 inhibits PTP activity

Several inhibitors of Shp2 have been identified from chemical libraries through in vitro high-throughput technologies.[44–46] However, these compounds are far from becoming treatments for cancer, and more potent inhibitors of Shp2 activity are needed. In recent years, a number of aptamers with excellent inhibitory effects on a variety of enzymes have been identified.[36,47,48] As the aptamer HJ24 binds to Shp2 with high affinity, we speculated on the possibility of the aptamer's inhibiting PTP activity in Shp2. The inhibitory effect of HJ24 on PTP activity was determined by using a phosphatase assay. As shown in Figure 7, HJ24 was able to inhibit Shp2 with an $IC_{50}$ as low as 29 nM, whereas the random sequence with the same length or the complementary DNA (cDNA) of HJ24 showed no inhibition of PTP activity. The results suggested that HJ24 is not only a good binder of Shp2, but also a good inhibitor of the PTP activity of Shp2. Recent efforts in the high-throughput screening of small-molecule inhibitors against PTP have identified many drug candidates with $IC_{50}$ values in the micromolar range.[49] In comparison, HJ24 has a much lower $IC_{50}$ value. With further optimization, HJ24 could be developed into effective therapies for the treatment of Shp2-dependent human malignancies and other diseases.

In addition to its high affinity and low $IC_{50}$, HJ24, as a single-stranded oligonucleotide, has another attractive advantage in that its inhibitory effect can be blocked by its cDNA. As the formation of secondary quadruplex structure is important to the binding of aptamer to its target, disruption of the secondary structure by its cDNA would lead to rapid and complete

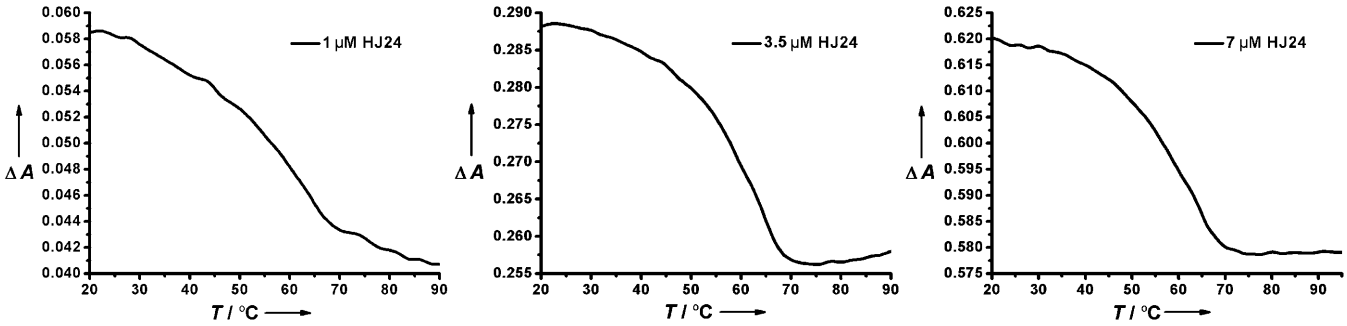


**Figure 5.** Denaturation profiles obtained at 295 nm for the aptamer at three different concentrations (1, 3.5, 7 μM). The $T_m$ (58 °C) at 295 nm is independent of oligonucleotide concentration; this indicates that the aptamer forms an intramolecular G-quadruplex.

  

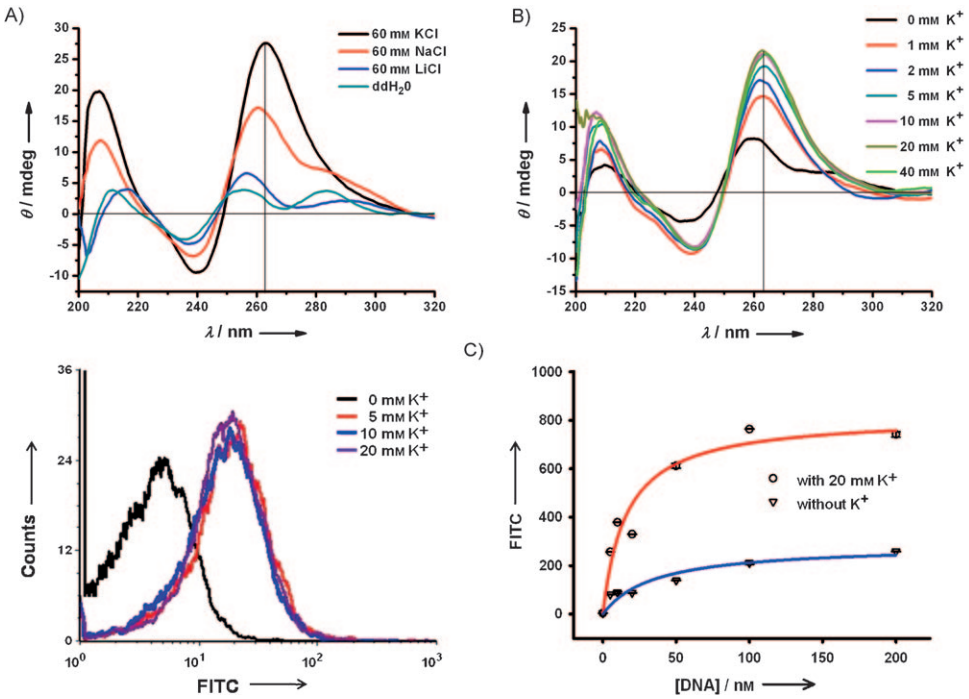


**Figure 6.** Effect of alkali metal ions on the structural stability of G-quadruplex HJ24 and its binding affinity. A) The relative effect of ions on the stability of the G-quadruplex is $K^+ > Na^+ > Li^+$. B) The structural stability of the aptamer relies heavily on $[K^+]$. C) The binding affinity of aptamer HJ24 also depends on $K^+$.

of cDNA, dephosphorylation activity was restored, as indicated by the increase in absorption. This experiment clearly demonstrated that our aptamer HJ24 and its cDNA can regulate the deactivation and activation of PTP phosphatase quickly and flexibly. The advantage of using HJ24 and its cDNA to rapidly and reversibly control PTP activity, together with its strong binding affinity, makes the aptamer a promising lead ligand for developing Shp2 inhibitors.

## Conclusions

In this work, we have developed new aptamer probes for specific recognition of the phosphatase Shp2. In the SELEX process, Shp2-GST fused protein was used as the target protein. Instead of using a conventional conjugation reaction, we linked

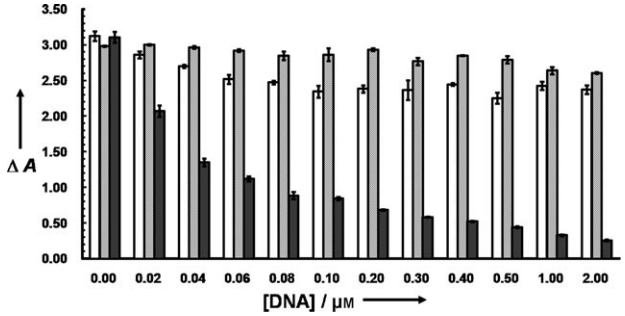


**Figure 7.** Inhibition effect of HJ24 on PTP activity. PTP activity was assayed by using *p*-nitrophenyl phosphate (*p*NPP) as a substrate. HJ24 (■) showed inhibition of PTP with an $IC_{50}$ value of 29 nM. In contrast, neither of the negative controls (random: □, cDNA: (■) inhibited PTP activity.

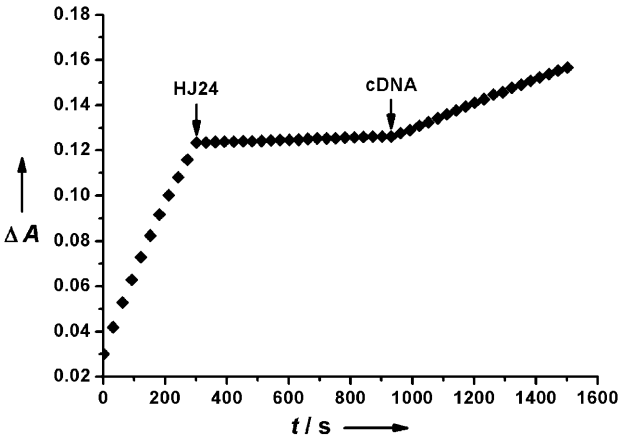


**Figure 8.** Reversible regulation of PTP activity by HJ24 and its cDNA.

deactivation of the aptamer's inhibition activity. There have been reports of applying cDNAs as effective inhibitors to deactivate therapeutic aptamers.[50–52] Such nucleic acid-based antidotes offer several advantages. Firstly, they are easy to synthesize with predictable toxicity profiles. Secondly, the binding of cDNA to aptamer is fast, thus the deactivation of aptamer activity is rapid. We explored whether the cDNA of HJ24 could regulate the activity of HJ24 and therefore Shp2 activity. As shown in Figure 8, Shp2 was added to a solution of the PTP substrate *p*-nitrophenyl phosphate (*p*NPP). The absorption of the solution increased as a result of the hydrolysis of the substrate catalyzed by PTP. When HJ24 was added, the absorption of the solution barely changed, thus indicating effective inhibition of PTP by HJ24. However, immediately after the addition of the Shp2-GST fused protein to Sepharose beads through the mild, yet specific, noncovalent GST–glutathione interaction. The hydrophilic nature of the Sepharose surface minimizes nonspecific binding of DNA to surfaces, thus ensuring systematic enrichment of target binding sequences. Bead-based SELEX allowed the use of simple, yet effective flow cytometry analysis to monitor the progress of the selection, avoiding the tedious, time consuming and radioactive EMSA process. Through multiple rounds of selection with GST as a control, we have identified two classes of aptamers that selectively recognize Shp2 with nanomolar $K_d$ values. CD measurements and melting temperature assays demonstrated that the optimal aptamer HJ24 forms a parallel G-quadruplex structure, which is

  

vital to the binding of HJ24 to its target. Moreover, HJ24 showed a strong inhibitory effect on Shp2 phosphatase activity and an $IC_{50}$ value of 29 nM. We further demonstrated that the inhibitory effect of HJ24 can be regulated in real time by its cDNA. This aptamer has great potential to serve as a tool to delineate the function of Shp2 phosphatase in normal physiology and under pathological conditions and as a lead ligand for the further development of novel therapeutics for the treatment of Shp2-dependent human malignancies and other diseases.

## Experimental Section

**Preparation of Shp2-GST fused protein:** The plasmid pGEX4T1-Shp2 (a gift from Dr. Gensheng Feng at the University of California San Diego) was transformed into the engineering strain BL-21 and the GST-tagged Shp2 protein was expressed. After purification with glutathione Sepharose beads (GE healthcare) by affinity chromatography, the Shp2-GST fused protein was linked to Sepharose beads for positive selection. After being washed several times with W1 buffer (25 mM Tris·HCl pH 7.5, 150 mM NaCl, 0.07% β-mercaptoethanol, 1% Triton X-100), the final purified Shp2-GST-beads were stored in sterilized phosphate buffered saline solution. Flow analysis with TAMRA-labled anti-Shp2 monoclonal antibody (Santa Cruz) and SDS-PAGE indicated that the Shp2-GST fused protein was successfully linked to the Sepharose beads. The number of Shp2-GST fusion protein molecules on each bead was estimated to be $3.7\times10^8$.

**Initial library design:** The aim of the SELEX experiment was to identify DNA sequences that specifically bind to Shp2 and to develop fluorescent probes targeting Shp2 or inhibitors against Shp2. The SELEX process was initiated by preparation of an initial library, consisting of a pool of oligonucleotides with a continuous stretch of 40 randomized nucleotides. The random sequences were flanked on both sides by fixed sequences used for the hybridization of PCR primers during subsequent rounds of amplification. SELEX library: 5′-AGC GTC GAA TAC CAC TAC AG-N40-CTA ATG GAG CTC GTG GTC AG-3′, forward primer: 5′-FAM-AGC GTC GAA TAC CAC TAC AG-3′, reverse primer: 5′-Bio-CTG ACC ACG AGC TCC ATT AG-3′. All of the oligonucleotides, including PCR primers, were synthesized in house using standard phosphoramidite chemistry and purified by RP-HPLC to remove the truncated DNA fragments produced in the chemical synthesis and finally desalted by using NAP-5 desalting columns (GE healthcare).

**Combinatorial selection of aptamer:** The procedures of selection were as follows. The ssDNA pool (200 pmol) dissolved in binding buffer (200 μL) was denatured by heating at 95 °C for 5 min, then quickly cooled on ice for 10 min, and subsequently incubated for another 10 min at room temperature before binding. The ssDNA pool was then incubated with GST beads (negative beads; $8.1\times10^4$ beads, $3.7\times10^9$ proteins per bead) for counter selection to remove sequences binding to GST beads. After filtering with a homemade filter column, the filtrate was incubated with positive Shp2-GST-beads ($8\times10^4$ beads, $3.7\times10^8$ proteins per bead) at 37 °C for 45 min. The partitioning step to separate the target-bound aptamers from the unbound or nonspecifically bound oligos was performed in the homemade filter column. The aptamers bound to the target-coated beads were then amplified by PCR with FAM- and biotin-labeled primers (5–15 cycles of 0.5 min at 94 °C, 0.5 min at 53 °C, and 0.5 min at 68 °C, followed by 5 min at 68 °C; the KOD plus polymerase and dNTPs were obtained from Toyobo, Osaka, Japan). After being denatured in NaOH (0.1 M), the selected sense ssDNA was separated from the biotinylated antisense ssDNA strand on streptavidin-coated Sepharose beads (GE healthcare) and used for next round selection. For the first-round selection, the amount of initial ssDNA pool was 5 nmol, dissolved in binding buffer (500 μL), and the counter-selection step was eliminated. To acquire aptamers with high affinity and specificity, the selection strength was enhanced gradually by increasing the number of washes (from three to five) and decreasing the ssDNA amounts of the library per round (from 200 to 160 pmol).

**Cloning and DNA sequencing:** The resulting pool from the 10th round was PCR amplified, cloned and sequenced (Shanghai Sangon sequencing facility). The resulting 48 sequences were subjected to multiple sequence alignment analysis by using Clustal W 6.0 software to discover highly conserved motifs in groups of selected DNA sequences. The discovered consensus sequences with high repeats among selected pools were then chemically synthesized on a DNA synthesizer (Polygen, Langen, Germany) for further testing.

**Flow cytometric analysis:** To monitor the enrichment of aptamers after selection, the FAM-labeled ssDNA pool was incubated with $8\times10^4$ Shp2-GST beads or GST beads in binding buffer (200 μL) at 37 °C for 45 min. Beads were washed three times with the binding buffer by means of filtering, and suspended in binding buffer (250 μL). The fluorescence was determined with a FACSAria cytometer (Becton Dickinson Immunocytometry systems) by counting 10000 events. The FAM-labeled unselected ssDNA library was used as a background. The binding affinities of aptamers were determined by incubating Shp2-GST beads ($5\times10^4$) with various concentrations of FAM-labeled aptamers (pre-heat-treated) in binding buffer (200 μL) at 37 °C for 45 min in the dark. Beads were then washed three times with the binding buffer by means of filtration, then resuspended in binding buffer (250 μL) and subjected to flow analysis. The FAM-labeled unselected ssDNA library was used as a negative control for the nonspecific binding. All binding experiments were repeated two to four times. The mean fluorescence intensity of target protein labeled by aptamers was used to evaluate binding affinity by subtracting the mean fluorescence intensity of nonspecific binding produced by unselected library DNAs. The dissociation constants ($K_d$) of the fluorescent ligands were obtained by fitting the dependence of fluorescence intensity of specific binding on the concentration of the ligands to the Equation (1):

$$Y = B_{max}X/(K_d + X)$$

by using the SigmaPlot software.

**Circular dichroism spectroscopy:** CD measurements were carried out on a Jasco J-810 spectropolarimeter equipped with a programmable temperature-control unit (Julabo HP-4). DNA samples were used at a concentration of 2 μM. Before the CD spectrum was obtained, the DNA samples were annealed by heating to 95 °C for 5 min and rapidly cooled on ice for 10 min, then incubated for another 10 min at room temperature. The spectra were obtained by using a 1 nm slit width and a scanning step of 0.1 nm from 400 to 200 nm. Each spectrum was an average of 8 scans with the buffer background subtracted.

**UV thermal-denaturation experiment:** UV absorbance and melting studies were carried out on an Agilent 8453 spectrophotometer equipped with a programmable temperature-control unit (Agilent 89090A). Melting temperatures ($T_m$) were taken as the temperature of half-dissociation of the quadruplex and were obtained from the maximum of the first derivative d*A*/d*T* plots at 295 nm.

  

The heat-treated DNA solutions at several concentrations were introduced into a quartz cuvette which was then covered with a thin layer of silicone oil to prevent evaporation. The optical path length was 1 cm. Absorbance and temperature were recorded every 2 °C.

**Determination of inhibition $IC_{50}$ value:** PTP activity was assayed by using *p*-nitrophenyl phosphate (*p*NPP) as a substrate in the reaction buffer (50 mM Bis-Tris, pH 6.5, 2 mM EDTA, 20 mM KCl, 2 mM DTT) at 25 °C. The assays were performed in 96-well plates. Typically, in order to determine the $IC_{50}$ values, the enzyme (200 nM) was incubated with various concentrations of HJ24 at room temperature for 30 min before adding *p*NPP (1.5 mM). The reaction was allowed to proceed for another 1 h and then quenched with NaOH (0.5 M). The absorbance at 405 nm was read on a microplate spectrophotometer (Thermo Multiskan MK3). $IC_{50}$ values were obtained by fitting data using SigmaPlot Enzyme Kinetics Module (Systat Software, Inc.). A scrambled 80-nt ssDNA sequence and HJ24 cDNA were used as negative controls.

## Acknowledgements

*This work was supported by the Natural Science Foundation of Fujian Province, China (2008J0107, 2010J06004), the National Scientific Foundation of China (20805038, 21075104, 30772546) and the National Basic Research Program of China (2007CB935603, 2010CB732402, 2010CB945004). We thank Dr. Gensheng Feng at the University of California San Diego for the gift of the plasmid pGEX4T1-Shp2.*

**Keywords:** aptamers · G-quadruplexes · inhibitors · phosphatases · SELEX

[1] P. Blume-Jensen, T. Hunter, *Nature* **2001**, *411*, 355 – 365.
[2] Z. Y. Zhang, *Curr. Opin. Chem. Biol.* **2001**, *5*, 416 – 423.
[3] S. Arena, S. Benvenuti, A. Bardelli, *Cell. Mol. Life Sci.* **2005**, *62*, 2092 – 2099.
[4] R. J. Chan, G. S. Feng, *Blood* **2007**, *109*, 862 – 867.
[5] B. G. Neel, H. H. Gu, L. Pao, *Trends Biochem. Sci.* **2003**, *28*, 284 – 293.
[6] J. M. Cunnick, S. S. Meng, Y. Ren, C. Desponts, H. G. Wang, J. Y. Djeu, J. Wu, *J. Biol. Chem.* **2002**, *277*, 9498 – 9504.
[7] H. Higashi, R. Tsutsumi, S. Muto, T. Sugiyama, T. Azuma, M. Asaka, M. Hatakeyama, *Science* **2002**, *295*, 683 – 686.
[8] E. Legius, C. Schrander-Stumpel, E. Schollen, C. Pulles-Heintzberger, M. Gewillig, J. P. Fryns, *J. Med. Genet.* **2002**, *39*, 571 – 574.
[9] M. L. Loh, S. Vattikuti, S. Schubbert, M. G. Reynolds, E. Carlson, K. H. Lieuw, J. W. Cheng, C. M. Lee, D. Stokoe, J. M. Bonifas, N. P. Curtiss, J. Gotlib, S. Meshinchi, M. M. Le Beau, P. D. Emanuel, K. M. Shannon, *Blood* **2004**, *103*, 2325 – 2331.
[10] M. Tartaglia, E. L. Mehler, R. Goldberg, G. Zampino, H. G. Brunner, H. Kremer, I. van der Burgt, A. H. Crosby, A. Ion, S. Jeffery, K. Kalidas, M. A. Patton, R. S. Kucherlapati, B. D. Gelb, *Nat. Genet.* **2001**, *29*, 465 – 468.
[11] M. Tartaglia, C. M. Niemeyer, A. Fragale, X. L. Song, J. Buechner, A. Jung, K. Hahlen, H. Hasle, J. D. Licht, B. D. Gelb, *Nat. Genet.* **2003**, *34*, 148 – 150.
[12] D. H. Christiansen, F. Desta, M. K. Andersen, J. Pedersen-Bjergaard, *Genes Chromosomes Cancer* **2007**, *46*, 517 – 521.
[13] J. Chen, W. M. Yu, H. Daino, H. E. Broxmeyer, B. J. Druker, C. K. Qu, *Blood* **2007**, *109*, 778 – 785.
[14] A. Östman, C. Hellberg, F. D. Bohmer, *Nat. Rev. Cancer* **2006**, *6*, 307 – 320.
[15] R. Nutiu, Y. F. Li, *Angew. Chem.* **2005**, *117*, 1085 – 1089; *Angew. Chem. Int. Ed.* **2005**, *44*, 1061 – 1065.
[16] D. S. Wilson, J. W. Szostak, *Annu. Rev. Biochem.* **1999**, *68*, 611 – 647.
[17] S. E. Osborne, A. D. Ellington, *Chem. Rev.* **1997**, *97*, 349 – 370.
[18] C. Tuerk, L. Gold, *Science* **1990**, *249*, 505 – 510.
[19] A. D. Ellington, J. W. Szostak, *Nature* **1990**, *346*, 818 – 822.
[20] C. Wu, J. Hu, Y. Zou, C. Wang, J. Liu, C. Yang, *Progress Chem.* **2010**, *22*, 1518 – 1530.
[21] D. Shangguan, Z. W. Tang, P. Mallikaratchy, Z. Y. Xiao, W. H. Tan, *ChemBioChem* **2007**, *8*, 603 – 606.
[22] S. D. Jayasena, *Clin. Chem.* **1999**, *45*, 1628 – 1650.
[23] X. H. Fang, W. H. Tan, *Acc. Chem. Res.* **2010**, *43*, 48 – 57.
[24] G. Mayer, *Angew. Chem.* **2009**, *121*, 2710 – 2727; *Angew. Chem. Int. Ed.* **2009**, *48*, 2672 – 2689.
[25] C. J. Yang, S. Jockusch, M. Vicens, N. J. Turro, W. H. Tan, *Proc. Natl. Acad. Sci. USA* **2005**, *102*, 17278 – 17283.
[26] E. J. Cho, J. W. Lee, A. D. Ellington, *Annu. Rev. Anal. Chem.* **2009**, *2*, 241 – 264.
[27] D. Shangguan, Y. Li, Z. W. Tang, Z. H. C. Cao, H. W. Chen, P. Mallikaratchy, K. Sefah, C. Y. J. Yang, W. H. Tan, *Proc. Natl. Acad. Sci. USA* **2006**, *103*, 11838 – 11843.
[28] C. C. Wu, L. Yan, C. M. Wang, H. X. Lin, C. Wang, X. Chen, C. J. Yang, *Biosens. Bioelectron.* **2010**, *25*, 2232 – 2237.
[29] S. H. Li, H. Xu, H. M. Ding, Y. P. Huang, X. X. Cao, G. Yang, J. Li, Z. G. Xie, Y. H. Meng, X. B. Li, Q. Zhao, B. F. Shen, N. S. Shao, *J. Pathol.* **2009**, *218*, 327 – 336.
[30] M. S. L. Raddatz, A. Dolf, E. Endl, P. Knolle, M. Famulok, G. Mayer, *Angew. Chem.* **2008**, *120*, 5268 – 5271; *Angew. Chem. Int. Ed.* **2008**, *47*, 5190 – 5193.
[31] Z. W. Tang, D. Shangguan, K. M. Wang, H. Shi, K. Sefah, P. Mallikratchy, H. W. Chen, Y. Li, W. H. Tan, *Anal. Chem.* **2007**, *79*, 4900 – 4907.
[32] Z. L. Zhao, L. Xu, X. L. Shi, W. H. Tan, X. H. Fang, D. H. Shangguan, *Analyst* **2009**, *134*, 1808 – 1814.
[33] H. W. Chen, C. D. Medley, K. Sefah, D. Shangguan, Z. W. Tang, L. Meng, J. E. Smith, W. H. Tan, *ChemMedChem* **2008**, *3*, 991 – 1001.
[34] D. H. Shangguan, L. Meng, Z. H. C. Cao, Z. Y. Xiao, X. H. Fang, Y. Li, D. Cardona, R. P. Witek, C. Liu, W. H. Tan, *Anal. Chem.* **2008**, *80*, 721 – 728.
[35] D. M. Tasset, M. F. Kubik, W. Steiner, *J. Mol. Biol.* **1997**, *272*, 688 – 698.
[36] K. T. Shum, J. A. Tanner, *ChemBioChem* **2008**, *9*, 3037 – 3045.
[37] R. F. Macaya, P. Schultze, F. W. Smith, J. A. Roe, J. Feigon, *Proc. Natl. Acad. Sci. USA* **1993**, *90*, 3745 – 3749.
[38] T. Simonsson, *Biol. Chem.* **2001**, *382*, 621 – 628.
[39] S. Burge, G. N. Parkinson, P. Hazel, A. K. Todd, S. Neidle, *Nucleic Acids Res.* **2006**, *34*, 5402 – 5415.
[40] J. T. Davis, *Angew. Chem.* **2004**, *116*, 684 – 716; *Angew. Chem. Int. Ed.* **2004**, *43*, 668 – 698.
[41] A. T. Phan, V. Kuryavyi, D. J. Patel, *Curr. Opin. Struct. Biol.* **2006**, *16*, 288 – 298.
[42] P. A. Rachwal, K. R. Fox, *Methods* **2007**, *43*, 291 – 301.
[43] J. L. Mergny, A. T. Phan, L. Lacroix, *FEBS Lett.* **1998**, *435*, 74 – 78.
[44] L. W. Chen, S. S. Sung, M. L. R. Yip, H. R. Lawrence, Y. Ren, W. C. Guida, S. M. Sebti, N. J. Lawrence, J. Wu, *Mol. Pharmacol.* **2006**, *70*, 562 – 570.
[45] X. Zhang, Y. T. He, S. J. Liu, Z. H. Yu, Z. X. Jiang, Z. Y. Yang, Y. S. Dong, S. C. Nabinger, L. Wu, A. M. Gunawan, L. N. Wang, R. J. Chan, Z. Y. Zhang, *J. Med. Chem.* **2010**, *53*, 2482 – 2493.
[46] K. Hellmuth, S. Grosskopf, C. T. Lum, M. Wurtele, N. Roder, J. P. von Kries, M. Rosario, J. Rademann, W. Birchmeier, *Proc. Natl. Acad. Sci. USA* **2008**, *105*, 7275 – 7280.
[47] A. Allali-Hassani, M. P. Pereira, N. K. Navani, E. D. Brown, Y. F. Li, *ChemBioChem* **2007**, *8*, 2052 – 2057.
[48] B. Townshend, I. Aubry, R. C. Marcellus, K. Gehring, M. L. Tremblay, *ChemBioChem* **2010**, *11*, 1583 – 1593.
[49] Z. X. Jiang, Z. Y. Zhang, *Cancer Metastasis Rev.* **2008**, *27*, 263 – 272.
[50] Z. H. Cao, R. Tong, A. Mishra, W. C. Xu, G. C. L. Wong, J. J. Cheng, Y. Lu, *Angew. Chem.* **2009**, *121*, 6616 – 6620; *Angew. Chem. Int. Ed.* **2009**, *48*, 6494 – 6498.
[51] J. Müller, D. Freitag, G. Mayer, B. Potzsch, *J. Thromb. Haemostasis* **2008**, *6*, 2105 – 2112.
[52] C. P. Rusconi, J. D. Roberts, G. A. Pitoc, S. M. Nimjee, R. R. White, G. Quick, E. Scardino, W. P. Fay, B. A. Sullenger, *Nat. Biotechnol.* **2004**, *22*, 1423 – 1428.

Received: November 12, 2010
Published online on January 10, 2011

  